Vol 15 No 6, June 2006
1009-1963/2006/15(06)/1268-05

Chinese Physics

© 2006 Chin. Phys. Soc.
and IOP Publishing Ltd

# Observation of four-wave mixing in caesium atoms using a noncycling transition*

Wang Li-Rong(汪丽蓉)†, Ma Jie(马 杰), Zhao Jian-Ming(赵建明),
Xiao Lian-Tuan(肖连团), and Jia Suo-Tang(贾锁堂)

*State Key Laboratory of Quantum Optics and Quantum Optic Devices, College of Physics and Electronic Engineering, Shanxi University, Taiyuan 030006, China*

(Received 11 November 2005; revised manuscript received 16 January 2006)

In this paper the generation of four-wave mixing (FWM) signal using a noncycling transition of caesium atoms is investigated when the pumping laser is locked to the transition $6S_{1/2}F = 4 \rightarrow 6P_{3/2}F' = 4$, and meanwhile the probe frequency is scanned across the $6S_{1/2}F = 4 \rightarrow 6P_{3/2}$ transition. The efficiency of the four-wave mixing signal as a function of the intensity of the pumping beams and the detuning of the pumping beams is also studied. In order to increase the detection efficiency, a repumping laser which is resonant with $6S_{1/2}F = 3 \rightarrow 6P_{3/2}F' = 4$ transition is used. A theoretical model is also introduced, and the theoretical results are in qualitative agreement with experimental ones.

**Keywords:** four wave mixing, caesium atom, noncycling transition
**PACC:** 3280,4250,4265

## 1. Introduction

Four-wave mixing (FWM) is the generation of a fourth field as a result of the interaction of three electromagnetic fields in a material sample, and this nonlinear optical generation process is allowed in all kinds of materials.[1,2] It has potential applications in optical image amplification and image processing. This effect has been studied also as an interesting subject in view of such important applications as third-harmonic generation and phase conjugation. Many experiments of FWM utilized an alkali metal vapour as the nonlinear medium and were carried out either in hot vapors,[3−7] or with cold atoms in a magneto-optical trap (MOT).[8,9] However, these experiments were mainly done using the cycling transition of the alkali atom.[10,11] It is well known that optical pumping prevents the observations of FWM signal in a noncycling transition, i.e., a transition which does not conserve the total population. Although Ai *et al*[12] demonstrated that frequent atom-wall collisions can overcome the effects of optical pumping when atomic vapors are contained in thin cells. In this paper, we find that introducing a repumping laser is a very appropriate way to observe FWM signal in noncycling transition.

In this paper, we present an investigation of FWM signal in caesium atoms using a noncycling transition by introducing a repumping laser, and the effects of frequency detuning and intensity of the pumping laser on the signal of FWM are experimentally investigated. The theoretical discussion is also made for qualitative explanation of these effects.

## 2. Experimental setup and results

The experiment is carried out on the $D_2$ transition of $^{133}$ Cs atoms. The energy level structure of the $^{133}CsD_2$ transition lines and FWM scheme is depicted in Fig.1.

The FWM laser fields (the forward pump (F), the backward pump (B), and the probe (P)) couple the Cs $6S_{1/2}F = 4 \rightarrow 6P_{3/2}$ transition. R is the repumping laser, which is resonant with the transition of $6S_{1/2}F = 3 \rightarrow 6P_{3/2}F' = 4$, to recycle the population loss to the hyperfine level $6S_{1/2}F = 3$ of the caesium

*Project supported by the National Natural Science Foundation of China (Grant No 60378004) and the Youth Science Foundation of Shanxi Province,China (Grant Nos 20031004 and 20041013).
†E-mail: wlr@sxu.edu.cn

ground state. The FWM signal is generated in the backward direction relative to the forward probe.

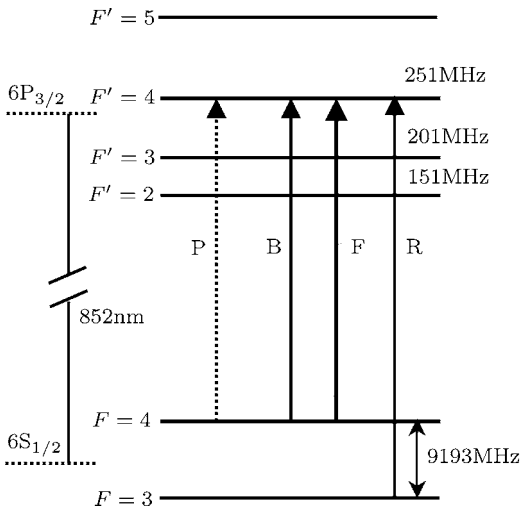



**Fig.1.** Relevant energy levels of Cs atom. F and B are the forward and backward pumping lasers, respectively; P denotes the probe lasers; R is repumping laser.

The experimental setup is schematically shown in Fig.2. The pumping laser is a frequency-stabilized Ti:sapphire laser (Coherent, MBR-110) of which the linewidth is less than 100 kHz when the frequency is stabilized to the $6S_{1/2}F = 4 \rightarrow 6P_{3/2}F' = 4$ transition by using a standard saturated absorption technology. It is used to produce the forward pumping and backward pumping beams. The forward pumping beam can be attenuated by a neutral density filter and then reflected back to form the backward pumping beam which is overlapped with the forward pumping beam. The angle between the forward pumping beam and the forward probe beam is about 10 mrad. The probe laser is an external cavity diode laser (New Focus, model 6017), which is temperature-stabilized and can be tuned on the $D_2$ line of caesium atoms. The free-running linewidth is less than 500 kHz ($< 50$ ms). The output of the probe laser is separated into two beams by a polarization beam splitter cube after

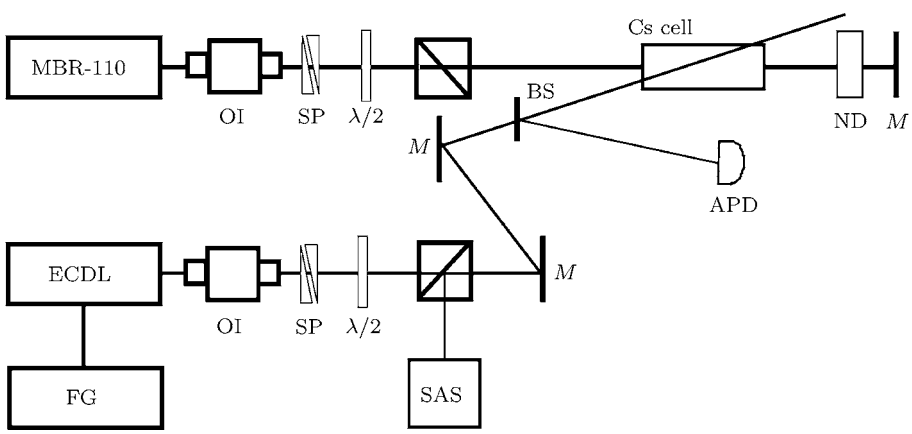



**Fig.2.** Experimental set-up. MBR-110 stands for Model MBR-110; Ti: sapphire laser; ECDL, external cavity diode laser; FG, function generator; OI, optical isolator; SP, shaping prism; SAS, saturated absorption spectrum; APD, avalanche photodiode; $M$: full reflection mirror; ND, neutral density filter.

passing through an optical isolator and an anamorphic pair of prisms. One beam is used to provide a frequency reference by saturated absorption in a caesium cell. The other beam is sent to another caesium cell and is used as the probe beam. The probe, the forward pumping and the backward pumping lasers are arranged to have same linear polarizations and propagate through a 5-cm-long caesium vapour cell kept at room temperature. The generated backward FWM signal is in the path of the probe beam and is detected by an avalanche photodiode (Hamamatsu Si APD, S3884) and recorded by a digital oscilloscope. The repumping laser is another external-cavity diode laser (New Focus, model 6017, not shown in Fig.2), the frequency of which is locked to the transition of $6S_{1/2}F = 3 \rightarrow 6P_{3/2}F' = 4$, this makes the population in the $6S_{1/2}F = 3$ level back to the $6S_{1/2}F = 4$ level.

The diameter of the probe beam is about 1mm, smaller than that of the pumping beam (about 3mm) in order to obtain a good overlapping. The probe beam in front of the caesium vapour is 0.8mW, while the power of the pumping beam can be changed with a polarizer, a $\lambda/2$ plate and a neutral density filter.

When the probe frequency is scanned across the $6S_{1/2}F = 4 \rightarrow 6P_{3/2}$ transition while the pumping

laser is stabilized to the transition $6S_{1/2}F = 4 \rightarrow 6P_{3/2}F' = 4$, the four wave mixing signal is observed. Due to the large hyperfine ground state splitting, the presence of the FWM beams around the noncycling transition $6S_{1/2}F = 4 \rightarrow 6P_{3/2}F' = 4$ leads to the increase of optical pumping rate to the non-interacting ground state $6S_{1/2}F = 3$, therefore results in a reduction in the observed signal. Introducing a "relaxation" mechanism that will redistribute the atoms between the ground states can eliminate this optical pumping problem. We will show that the presence of the repumping beam can be used to optically pump atoms from the non-interaction to the interaction ground state and make the observation of FWM signal in the noncycling transition possible. The result is shown in Fig.3, curve *a*. For this spectrum the power of the forward, backward and probe beams are $P_F \approx 60$mW, $P_B \approx 40$mW and $P_p \approx 0.8$mW respectively. The power of repumping laser is 5.2 mW (the diameter of the repumping laser beam is about 2 mm). In curve *a*, the two peaks are associated with the cycling transition $6S_{1/2}F = 4 \rightarrow 6P_{3/2}F' = 5$ and

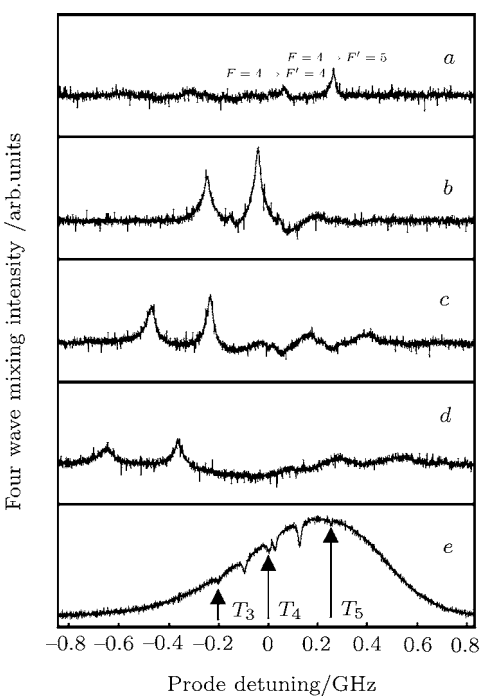



**Fig.3.** The FWM signal for various pumping detunings. The pumping intensity is 60mW and the diameter is about 3mm. The pumping laser is tuned to $6S_{1/2}$ $F = 4 \rightarrow 6P_{3/}F' = 4$ noncycling transition with a detuning of 0, -250, -450 and -650MHz for curves $a, b, c, d$, respectively. Curve $e$ is the saturated absorption spectrum.

the noncycling transition $6S_{1/2}F = 4 \rightarrow 6P_{3/2}F' = 4$ separately. The signal around the noncycling transitions is much smaller than the signal at the cycling transition due to the optical pumping.

As we have mentioned, the repumping laser plays an essential role for the observation of FWM around the noncycling transition. We can use a simple rate equation model to calculate the populations $N_{F=3}$ and $N_{F=4}$ of the two hyperfine ground states $6S_{1/2}F = 3$ and $6S_{1/2}F = 4$. [13] If $R_r$ and $R_d$ represent the repumping rate and the optical pumping rate, we obtain

$$\frac{N_{F=4}}{N_{F=3}} = \frac{R_r \tau_{F=4}}{R_d \tau_{F=3}}, \tag{1}$$

where $\tau_{F=4}$ and $\tau_{F=3}$ are the corresponding lifetimes of the ground state levels. If we assume that the total population of atoms $N_0 = N_{F=3} + N_{F=4}$ is constant, the intensity of FWM signal around the noncycling transition is given by

$$I_{NC} \propto N_0^2 \left( \frac{R_r}{R_r + R_d} \right)^2. \tag{2}$$

We use this simple model to analyse the dependence of the FWM signal in noncycling transition on the intensity of the repumping laser in the experiment. We find that the FWM signal reaches saturation when the power of repumping laser is 5.2 mW.

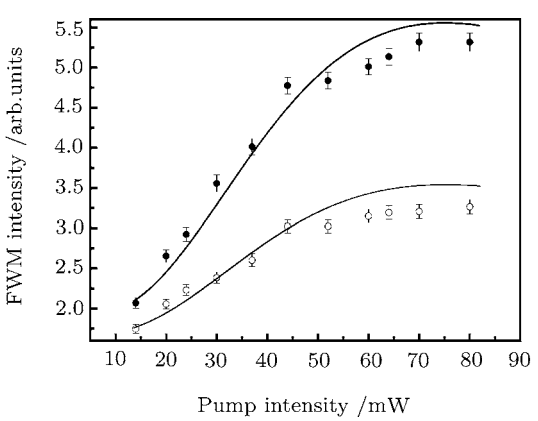



**Fig.4.** Dependence of FWM signal as a function of the pumping laser intensity. •-cycling transition ($6S_{1/2}F = 4 \rightarrow 6P_{3/2}F' = 5$); ○-noncycling transition($6S_{1/2}F = 4 \rightarrow 6P_{3/2}F' = 4$). The solid curve corresponds to the fitting using the dependence predicted by Eq.(8).

The effect of detuning of the pumping laser on the FWM signal is also investigated experimentally, and the experimental result is shown in Fig.3. The probe frequency is scanned across the $6S_{1/2}F = 4 \rightarrow 6P_{3/2}$ transition while the pumping laser is tuned to $6S_{1/2}F = 4 \rightarrow 6P_{3/2}F' = 4$ noncycling transition with the detuning of 0,–250,–450 and –650 MHz for

curves $a, b, c, d$, respectively. Curve $e$ is the saturated absorption spectrum. $T_3$,$T_4$,$T_5$ in curve $e$ indicate three resonant transitions from the ground-state hyperfine level $6S_{1/2}F = 4$ to the excited-state hyperfine level $6P_{3/2}$ with $F' = 3, 4, 5$, respectively. The intensity of the FWM signal is increased and the position of the FWM signal shifts with the red detuning of pumping laser increasing. But when the detuning of the pumping laser from the transition resonance $6S_{1/2}F = 4 \rightarrow 6P_{3/2}F' = 4$ is greater than the Doppler width, the FWM intensity decreases. We can obtain the same results from the following equation (8).

The dependence of FWM signal on the pumping power is shown in Fig.4 for both types of transitions, i.e. the cycling transition $6S_{1/2}F = 4 \rightarrow 6P_{3/2}F' = 5$ and the noncycling transition $6S_{1/2}F = 4 \rightarrow 6P_{3/2}F' = 4$.The probe frequency is scanned across the $6S_{1/2}F = 4 \rightarrow 6P_{3/2}$ transition while the pumping laser is stabilized to the transition $6S_{1/2}F = 4 \rightarrow 6P_{3/2}F' = 4$. The power of probe beam and the repumping are 0.8 mW and 5.2 mW, respectively. We change the forward pumping power and obtain the FWM signals. The FWM signals have analogous behaviours for the cycling and noncycling transitions. At low pumping power the signal around the noncycling transition is smaller than that of the cycling transition. When the pumping power increases, both the FWM intensities of noncycling transition and cycling transition increase, but FWM intensity around the cycling transition increases more quickly. At the high pumping intensity, the nonlinear behaviour indicates that the saturation of the third-order susceptibility $\chi^{(3)}$ occurs. This observed saturation is due to the participation of all the atoms in the FWM process. From the data of the experiment, it is obviously seen that the FWM signal of noncycling transition saturates before the signal of the cycling transition is getting to the saturation.

The observed FWM signal can be explained in terms of the density matrix equations. [14] Considering a two-level system consisting of ground state $|g\rangle(6S_{1/2}F = 4)$ and excited state $|e\rangle(6P_{3/2}F' = 4)$, which is driven by a pumping field $E_c$ of frequency $\omega_c$ and a probe field $E_p$ of frequency $\omega_p$, both of the two lasers are tuned near the atomic resonance. The Hamiltonian of this system is:

$$H = H_0 + H_{\rm Int}, \tag{3}$$

$$H_{\rm Int} = \mu_{\rm eg}\Big(E_c e^{-i\omega_c t} + E_p e^{-i\omega_p t})|e\rangle\langle g| + \text{c.c.}, \tag{4}$$

where $\mu_{\rm eg}$ is the dipole matrix element.

The Liouville equation for the matrix element can be written as

$$i\hbar\frac{\partial\rho}{\partial t} = [H_0, \rho] + [H_{\rm Int}, \rho] + i\hbar\frac{\partial\rho_{\rm damping}}{\partial t}. \tag{5}$$

In steady state the off diagonal density-matrix element $\rho_{\rm eg}$ exhibits harmonic oscillations at an infinite number of frequencies of the form $n\omega_c + m\omega_p$, where $n$ and $m$ are integers. We treat the pump field to all orders in $E_c$ and the probe field to the first order in $E_p$. $\rho_{\rm eg}$ can be expanded as a series of its Fourier components. If only the single-photon and three-photon processes are considered, $\rho_{\rm eg}$ is dominated by three main frequencies: $\omega_c$, $\omega_p$ and $2\omega_c - \omega_p$.

$$\begin{aligned}\rho_{\rm eg} =& \rho_{\rm eg}(\omega_c)e^{-i\omega_c t} + \rho_{\rm eg}(\omega_p)e^{-i\omega_p t} \\ &+ \rho_{\rm eg}(2\omega_c - \omega_p)e^{-i(2\omega_c - \omega_p)t}.\end{aligned} \tag{6}$$

The population inversion is also expanded into corresponding Fourier components as

$$\begin{aligned}\rho_{\rm ee} - \rho_{\rm gg} =& (\rho_{\rm ee} - \rho_{\rm gg})^0 \\ &+ (\rho_{\rm ee} - \rho_{\rm gg})^{(\omega_p - \omega_c)}e^{-i(\omega_p - \omega_c)t}.\end{aligned} \tag{7}$$

In steady state the Fourier FWM amplitudes can be obtained through a set of closed linear equations.

$$\rho_{\rm eg}(2\omega_c - \omega_p) = -\frac{\mu_{\rm ba}\Omega^2 E_p^*(\rho_{\rm ee} - \rho_{\rm gg})^{\rm dc}(2i\gamma_{\rm eg} - \delta)}{2\hbar[(i\gamma - \delta)(\Delta + i\gamma_{\rm eg} - \delta)(i\gamma_{\rm eg} - \Delta - \delta) - \Omega^2(i\gamma_{\rm eg} - \delta)](\Delta - i\gamma_{\rm eg})}, \tag{8}$$

where $(\rho_{\rm ee} - \rho_{\rm gg})^{\rm dc}$ is the steady state saturated population inversion induced by the pump field $E_c$.

$$(\rho_{\rm ee} - \rho_{\rm gg})^{\rm dc} = \frac{(\rho_{\rm ee} - \rho_{\rm gg})^0(1 + \Delta^2/\gamma_{\rm eg}^2)}{1 + \Delta^2/\gamma_{\rm eg}^2 + \Omega^2/\gamma\gamma_{\rm eg}}. \tag{9}$$

$\Omega$ is the Rabi frequency of the pumping field, $\Omega^2 = \frac{4|\mu_{\rm eg}|^2|E_c|^2}{\hbar^2}$, $\delta$ is the detuning of the pump-probe fields, $\Delta$ is the detuning of the pump from the resonance. $\gamma$ and $\gamma_{\rm eg}$ are the longitudinal and transverse decay rates, respectively. $(\rho_{\rm ee} - \rho_{\rm gg})^0$ is the equilibrium population inversion in the absence of the optical fields. The solid curve in Fig.4 is the theoretical re-

sults obtained from Eq.(8). It can be seen that the experimental results agree well with the theoretical calculations when the pumping intensity is low, but the saturation value of experimental results is smaller in comparison with the theoretical calculation value. This is due to the decrease of response of the detection system for high pumping intensity in the experiment.

## 3. Conclusion

In summary, we have investigated the generation of FWM in caesium atoms using a noncycling transition. The effect of the intensity and the detuning of pumping laser on FWM were studied experimentally. In order to reduce the pumping effect of the coupling laser, a repumping laser which was resonant with $6S_{1/2}F = 3 \rightarrow 6P_{3/2}F' = 4$ transition was introduced. A simple theoretical model using a two-level system was presented to explain the observed result.

## References


[1] Bloembergen N 1965 *Nonlinear Optic* (Benjamin, New York) Li X Z, Su B X and Chai L 2005 *Chin. Phys.* **14** 1833
Li J H, Luo J M, Yang W X and Peng J C 2005 *Chin. Phys.* **14** 990

[2] Shen Y R 1984 *The Principles of Nonlinear Optics* (New York: Wiley)
Fan R W, Chen D Y, Fang T, Ju Y L, Wang Q and Ma Z G 2004 *Chin. Phys.* **13** 700
Zhang Y L, Jiang L, Sun Z R, Ding L E and Wang Z G 2003 *Chin. Phys.* **12** 174

[3] Liao P F , Bloom D M and Economou N P 1978 *Appl. Phys. Lett.* **32** 813

[4] Bloch D , Raj RK, Peng KS and Ducloy M 1982 *Phys. Rev. Lett.* **49** 719

[5] Bermman P R, Steel D G, Khitrova G and Liu J 1988 *Phys. Rev.* A **38** 252

[6] Zhu Y F, Wang S J and mulchan N M 1999 *Phys. Rev.* A **59** 4005

[7] Li Y Q and Xiao M 1996 *Opt. Lett.* **21** 1064

[8] Durrant A V, Chen H X, Hopking S A and Vaccaro J A 1998 *Opt. Commun.* **151** 136

[9] Cadoso G C and Tabasa J W R 2002 *Phys. Rev.* A **65** 033803

[10] Lounis B, Vererk P , Courtois J Y, Salomon C and Gryberg G 1993 *Europhys. Lett.* **21** 13

[11] Hemmerich A, Weidemuller M and Hansch T 1994 *Europhys. Lett.* **27** 427

[12] Ai B, Grassner D S and Knize R J 1994 *Phys. Rev.* A **50** 3345

[13] Townsend C G, Edwards N H, Zetie K P, Cooper C J, Rink J and Foot C J 1996 *Phys. Rev.* A **53** 1702
Tabosa J W R and Vianna S S 1997 *Brazilian J. Phys.* **27** 243

[14] Boyd. R w, Raymer M G, Narum P and Harter D J 1981 *Phys. Rev.* A **24** 411